ELSEVIER

Journal of Molecular Catalysis A: Chemical 195 (2003) 219–223

JOURNAL OF MOLECULAR CATALYSIS A: CHEMICAL

www.elsevier.com/locate/molcata

# Polymer frameworks as templates for generating size-controlled metal nanoclusters Active and reusable metal catalysts based on organic resins and on organic/inorganic composites

M. Kralik [a,*], V. Kratky [a], P. Centomo [b], P. Guerriero [c], S. Lora [d], B. Corain [e,1]

[a] *Department of Organic Technology, Slovak University of Technology, Radlinskeho 9, 812 37 Bratislava 1, Slovak Republic*
[b] *Dipartimento di Chimica Inorganica Metallorganica Analitica, Via Marzolo 1, 35131 Padova, Italy*
[c] *Istituto di Chimica Inorganica e dei Materiali, C.N.R., Corso Stati Uniti 4, 35127 Padova, Italy*
[d] *Istituto F.R.A.E., C.N.R., Via Romea 4, 35020 Legnaro, Italy*
[e] *Istituto di Scienze e Tecnologie Molecolari, C.N.R., Sezione di Padova c/o Dipartimento di Chimica Inorganica Metallorganica Analitica, Via Marzolo 1, 35131 Padova, Italy*

Received 2 July 2002; accepted 15 October 2002

**Abstract**

Catalysts based on Pd nanoparticles supported on polyacrylic resins or on polyacrylic resins/silica composites are evaluated in terms of catalyst reusability and mechanical stability. Both technologically relevant features are satisfactory. Resin/silica/Pd composites exhibit an appreciable but not dramatic decrease of specific catalytic activity (3–4 times) when compared with their parent resin/Pd materials, but this decrease is compensated by higher mechanical stability and easier separability of the catalyst from the reaction mixture.


*Keywords:* Resin-supported Pd catalysts; Catalyst reusability; Mechanical stability

## 1. Introduction

In recent years, we have been working in developing the scientific bases of interesting and promising industrial metal catalysts based on ion-exchange resins, both macroreticular and of gel-type in nature (Bayer catalysts) [1–3]. In the course of our endeavor, we have developed efficient metallation and reduction protocols as well as a procedure suitable for controlling the allocation (peripheral versus full body) of the metal nanoclusters inside the resins particles [4]. We have also addressed in quantitative terms the crucial question of nanomorphology and molecular accessibility of the polymer framework [5,6] and we could conclude that lightly cross-linked (2–6 mol%) resins offer only a moderate resistance to mass transfer of reagents and products. Finally, we have also addressed the issue of chemical stability of the polymer framework under hydrogenation conditions (20–40 °C and 1–5 atm of dihydrogen) for reasonably long lasting operational times [7].

* Corresponding author. Fax: +421-2-5249-3198.
*E-mail addresses:* kralik@chtf.stuba.sk (M. Kralik), benedetto.corain@unipd.it (B. Corain).
[1] Co-corresponding author. Fax: +49-827-5223.

1381-1169/02/$ – see front matter © 2002 Elsevier Science B.V. All rights reserved.
PII: S1381-1169(02)00620-9

In the frame of our most recent work, we have also discovered that our gel-type resins [8] with cross-linking degree from 2 to 6 mol%, act as template structures in controlling the growth of palladium nanoparticles generated in their interior that turn out to exhibit a diameter always very near to 3 nm. Quite remarkably the same size appears to feature palladium nanoclusters generated at the "walls" of the macropores of a commercial macroreticular resin that we investigated for purposes not related to this apparent size-control effect [9].

We report here on a further step of our endeavor, i.e. an attempt to increase the mechanical stability of our catalysts upon re-inforcing our organic frameworks with a silica skeleton [10].

## 2. Results and discussion

The employed catalysts SPIM-$Na^+/Pd^0$, MPIF-$Na^+/Pd^0$, MPIF-$Na^+/Pd^0/SiO_2$ and SPIM-$Na^+/Pd^0/SiO_2$ were prepared according to [7,10,11]. Catalytic experiments were carried out with a pressostatic reactor described in [12]. All evaluated catalysts are dimethylacrylamide polymers cross-linked with methylenebisacrylamide (4 mol%) and therefore after the reduction with sodium borohydride they rest on aliphatic chains with either $–C(O)N(Me_2)$, –Me, $–C(O)–O–(CH_2)_2–SO_3^-Na^+$ or $–C(O)O^-Na^+$ as pendants (Fig. 1)

SPIM-$Na^+/Pd^0$ is a resin-supported catalyst described in [7] (Pd = 1.73%) and MPIF-$Na^+/Pd^0$ (Pd = 2.54%) is an analogous material described in [11]. SPIM-$Na^+/Pd^0/SiO_2$ (Pd = 0.9%) (10) and MPIF-$Na^+/Pd^0/SiO_2$ (Pd = 1.21%) [10] are very peculiar organic/inorganic composite formed by the entanglement of the polymer framework of MPIF-$Na^+/Pd^0$ or of SPIM-$Na^+/Pd^0$ and that of amorphous silica. They exhibit quite similar overall physico-chemical features. The organic/inorganic composites exhibit a nicely homogeneous distribution of silicon (XRMA) (resolution power is ca. 5 μm). For MPIF-$Na^+/Pd^0/SiO_2$ see [10] and for SPIM-$Na^+/Pd^0/SiO_2$ see Fig. 2.

XRMA reveals us that the entanglement of the organic and inorganic frameworks is extended to the entire body of the host matrix at least at the micrometer level.

Hydrogenation of cyclohexene catalyzed by SPIM-$Na^+/Pd^0$, MPIF-$Na^+/Pd^0$, SPIM-$Na^+/Pd^0/SiO_2$, MPIF-$Na^+/Pd^0/SiO_2$. Three consecutive runs for each tested catalyst were carried out to control catalyst stability. Catalyst are recycled upon careful decantation *under dihydrogen of the solution* obtained at the end of each test. The operation turns out to be amazingly facile for the $SiO_2$-loaded catalysts, apparently thanks to the higher density of these materials. Data are collected in Figs. 3 and 4. The independent variable is normalized upon multiplying the given time by the mass of the catalyst. This normalization comes out from the assumption that external mass transport is not rate limiting, i.e. that the rate of hydrogenation is linearly proportional to the mass of the catalyst itself. SPIM-$Na^+/Pd^0$ and MPIF-$Na^+/Pd^0$ exhibit almost identical normalized activity under seemingly diffusion-control and their reusability is perfect (Figs. 3 and 4; Table 1).

Both catalysts SPIM-$Na^+/Pd^0/SiO_2$ and MPIF-$Na^+/Pd^0/SiO_2$ exhibit a peculiar and rather similar reaction profile. In both the cases, the first runs display

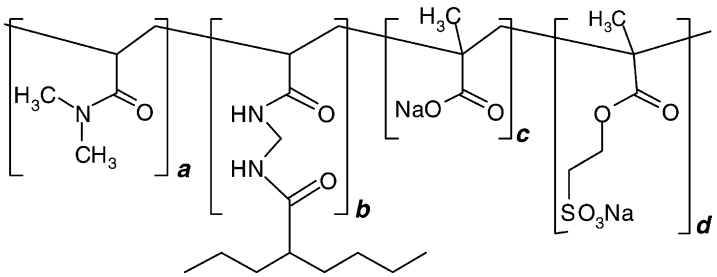


Fig. 1. Primary structure of the polymer chains in catalysts SPIM-$Na^+/Pd^0$ (composition in mol%) ($a = 92$, $b = 4$; $c = 0$; $d = 4$) and MPIF-$Na^+/Pd^0$ ($a = 88$; $b = 4$; $c = 8$; $d = 0$).

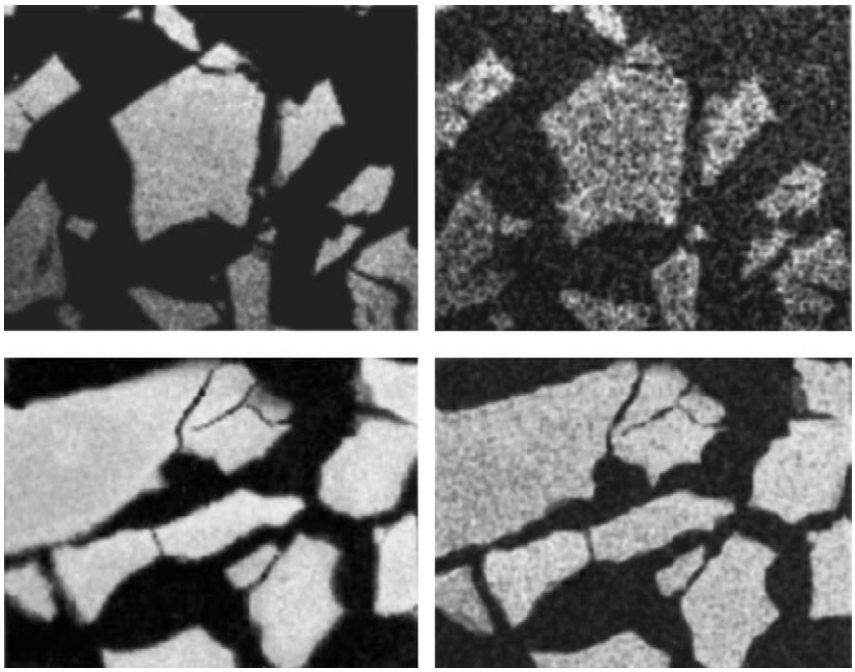

Fig. 2. XRMA maps for silicon (left) and palladium (right) of SPIM-$Na^+/Pd^0/SiO_2$ (top) and MPIF-$Na^+/Pd^0/SiO_2$ (bottom). Notice the homogeneous distribution of Si and Pd, lower quality of the Pd map for SPIM-$Na^+/Pd^0/SiO_2$ is due to low content of palladium. Particles are from the sieve fraction 0.18–0.4 mm. Cambridge Stereoscan 250 EDX PW9800.

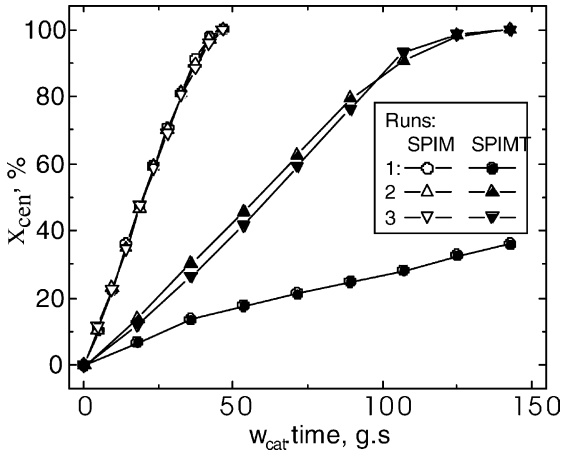


Fig. 3. Conversion ($X_{cen}$) of cyclohexene vs. time multiplied by the weight of the catalyst ($w_{cat}$ × time) in three consecutive runs over the SPIM-$Na^+/Pd^0$ catalyst (SPIM, open symbols) and SPIM-$Na^+/Pd^0/SiO_2$ (SPIMT, filled symbols). Weight of the catalyst: 0.1294 and 0.24805 g of SPIM-$Na^+/Pd^0$ catalyst and SPIM-$Na^+/Pd^0/SiO_2$, respectively; 6 ml of the reaction mixture consisting of methanol, cyclohexane and cyclohexene; 1 M cyclohexene at the start; 0.5 ± 0.05 MPa; 27 °C; shaking frequency: 6 Hz.

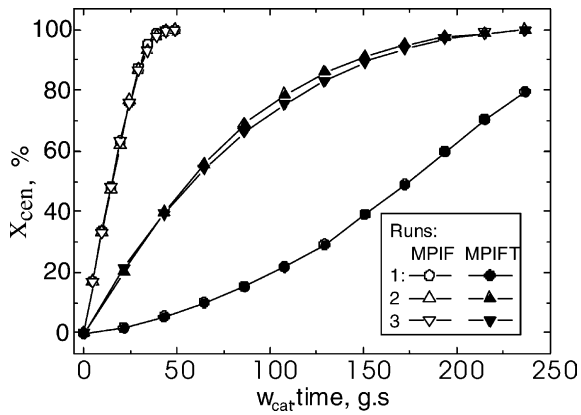


Fig. 4. Conversion ($X_{cen}$) of cyclohexene vs. time multiplied by the weight of the catalyst ($w_{cat}$ × time) in three consecutive runs over the MPIF-$Na^+/Pd^0$ catalyst (MPIF, open symbols) and MPIF-$Na^+/Pd^0/SiO_2$ (MPIFT, filled symbols). Weight of the catalyst: 0.08148 and 0.1793 g of MPIF-$Na^+/Pd^0$ catalyst and MPIF-$Na^+/Pd^0/SiO_2$, respectively; 6 ml of the reaction mixture consisting of methanol, cyclohexane and cyclohexene; 1 M cyclohexene at the start; 0.5 ± 0.05 MPa; 27 °C; shaking frequency: 6 Hz.

Table 1
Initial rates ($\xi_{cat}$, $\xi_{Pd}$) in the hydrogenation of cyclohexene over the investigated catalysts

| Catalyst | $\xi_{cat}$ ($\times 10^3$; $mol_{cen}/(g_{cat}\ s)$)[a] | $\xi_{Pd}$ ($\times 10^3$; $mol_{cen}/(g_{Pd}\ s)$) |
|---|---|---|
| SPIM-$Na^+/Pd^0$ | 0.165 | 9.55 |
| SPIM-$Na^+/Pd^0/SiO_2$ | 0.053 | 5.95 |
| MPIF-$Na^+/Pd^0$ | 0.215 | 8.46 |
| MPIF-$Na^+/Pd^0/SiO_2$ | 0.058 | 4.8 |

[a] Derived from tangents at points [0, 0] to the conversion curves in Figs. 3 and 4.

a sluggish activity that turns to a much larger one already with the first recycling. In addition, second and third runs turn out to be almost superimposable.

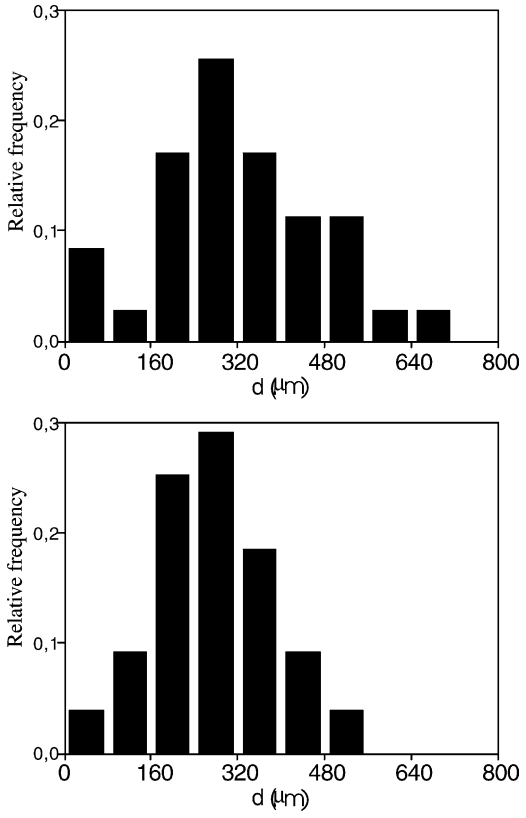


Fig. 5. Relative size distribution for the MPIF-$Na^+/Pd^0$ catalyst particles before (top, 35 particles) and after catalytic tests (bottom, 75 particles). Arithmetic average diameters 319 and 276 mm were determined for particles before and after catalytic tests, respectively. Image Pro Plus Program.

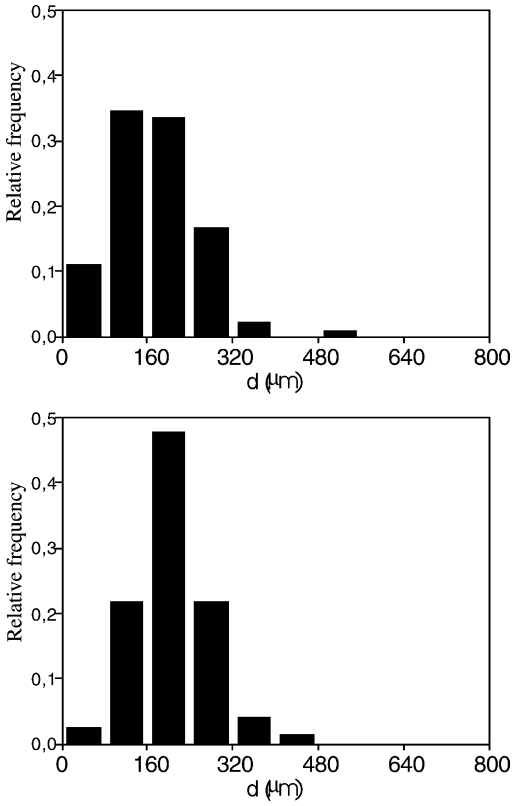


Fig. 6. Relative size distribution for the MPIF-$Na^+/Pd^0/SiO_2$ catalyst particles before (top, 89 particles) and after catalytic tests (bottom, 119 particles). Arithmetic average diameters 169 and 204 mm were determined for particles before and after catalytic tests, respectively. Image Pro Plus Program.

After this quite positive evaluation of chemical stability, we addressed the technologically important question of catalyst particles stability under operational conditions. The results are illustrated for the MPIF-$Na^+/Pd^0/SiO_2$ catalyst (Figs. 5 and 6).

The data are amazing. Both MPIF-$Na^+/Pd^0$ and SPIM-$Na^+/Pd^0/SiO_2$, MPIF-$Na^+/Pd^0/SiO_2$ catalysts result to be perfectly stable after three catalytic runs. These results are in fact very important in the light of technological prospects offered by resin-based metal catalysts [13]. Although the duration of the "mechanical" might be judged relatively short, the kinetic energy transferred to catalyst particles by the very vigorous agitation is estimated to be considerable enough to permit positive conclusions, in terms of catalysts mechanical stability.

## 3. Experimental

Solvents and chemicals were of reagent grade. Catalysts were prepared according to the following references: SPIM-$Na^+/Pd^0$ [7]; MPIF-$Na^+/Pd^0$ [11]; SPIM-$Na^+/Pd^0/SiO_2$ and MPIF-$Na^+/Pd^0/SiO_2$ [10].

*Apparatus*: SEM and XRMA, Cambridge Stereoscan 250 EDX PW9800; image analysis was carried out with a Image Pro Plus Program.

Catalytic experiments were carried out with a pressostatic reactor described in [12].

## Acknowledgements

This work was partially supported by PRIN Funding, 2001–2003, Ministero dell'Università e della Ricerca Scientifica, Italy (Project number 2001038991) and by the Slovak VEGA Project number 1/9142/02.

## References

[1] R. Wagner, P.M. Lange, Erdöl Erdgas Kohle 105 (1989) 414.
[2] P.M. Lange, F. Martinola, S. Oeckel, Hydrocarbon Process. December (1985) 51, and references therein.
[3] D.C. Sherrington, Chem. Commun. (1998) 2275.
[4] M. Králik, M. Hronec, S. Lora, G. Palma, M. Zecca, A. Biffis, B. Corain, J. Mol. Catal. A 97 (1995) 145.
[5] A. Biffis, B. Corain, M. Zecca, C. Corvaja, K. Jerabek, J. Am. Chem. Soc. 117 (1995) 1603.
[6] A.A. D'Archivio, L. Galantini, A. Panatta, E. Tettamanti, B. Corain, J. Phys. Chem. B 102 (1998) 6779, and references therein.
[7] M. Kralik,V. Kratky, M. De Rosso, M. Tonelli, S. Lora, B. Corain, Chem. Eur. J., in press.
[8] A. Biffis, A.A. D'Archivio, K. Jeràbek, G. Schmid, B. Corain, Adv. Mater. 12 (2000) 1909.
[9] A. Biffis, H. Landes, K. Jeràbek, B. Corain, J. Mol. Catal. A: Chem. 151 (2000) 283.
[10] B. Corain, P. Guerriero, G. Schiavon, M. Zapparoli, M. Kralik, Adv. Mater., submitted for publication.
[11] F. Artuso, A. A. D'Archivio, S. Lora, K. Jerabek, M. Kralik, B. Corain, Adv. Mater., submitted for publication.
[12] M. Hronec, J. Ilavsky, Chem. Papers 39 (1985) 705.
[13] B. Corain, M. Kralik, J. Mol. Catal. A: Chem. 159 (2000) 153.